

New Type of Oversaturated Superconducting Machine

Anis Smara^{1, *}, Abderrezak Rezzoug², Jean Lévêque², and Rachid Ibtouen¹

Abstract—This paper presents the principle and design of an experimental bench of an inductor of an oversaturated superconducting machine with radial flux density. A designed experimental bench is under construction to validate the computation and the principle of the inductor. Also, this work describes the encountered problems and lays out the tools that permit to study a high power oversaturated superconducting machine.

1. INTRODUCTION

The properties of superconductors, such as high current density, diamagnetic behavior and magnetic flux trapping, opened the door to large possibilities in terms of electrical machines design [1–6]. Their feasibility, however, is not trivial because of many constraints imposed by such materials.

To build a simple coil we can mention, without being exhaustive, the constraints ($T < T_c$, $J < J_c$, $B < B_c$) which must be respected in any point of the superconductor. For the mechanical constraints, we note the limited curvature radius $> R_{c-\min}$ and the forces applied on the superconductor.

As a consequence, the calculation of any superconducting machine is more difficult than that of any conventional one which benefits from more than a hundred years of industrial experience. Taking into account the experience in the domain, we can affirm that superconducting machines can be competitive in the area of large power machines. Within this frame, earlier we proposed an original structure of an oversaturated machine with an axial magnetic flux spatially modulated in the angular direction, and we also proposed a scheme of a machine, based on the same principle, in which a radial flux density is used [7, 8].

This paper presents a work developed to verify and illustrate the principle of a radial oversaturated machine by studying the air gap flux density distribution created by an oversaturated radial inductor. After the presentation of the principle and general scheme, design of the inductor is made. The design of the future experimental bench is analyzed.

2. BASIC PRINCIPLE OF AN OVERSATURATED MACHINE

The magnetic moments of a ferromagnetic piece, plunged in a high magnetic field, are oriented along the flux lines of this field. The magnetic flux inside the material can be expressed as:

$$\vec{B} = \mu_0(\vec{H} + \vec{M}) \quad (1)$$

where B , μ_0 , H , and M represent the magnetic flux density (T), magnetic vacuum permeability (H/m), magnetic field (A/m), and magnetization (A/m), respectively.

Equation (1) is valid for all ferromagnetic materials and for all values of the magnetic field. However, increasing the external magnetic field will increase the value of magnetization M . If the external field

Received 9 June 2017, Accepted 28 August 2017, Scheduled 6 October 2017

* Corresponding author: Anis Smara (anisenp@gmail.com).

¹ Ecole Nationale Polytechnique (LRE-ENP), Algiers, 10, Av. Pasteur, El Harrach, BP 182, 16200, Algeria. ² Green, Faculte des Sciences et Technologies, BP 70239, 54506 Vandoeuvre les Nancy, France.

is high enough, and as long as it is present, the ferromagnetic material will be saturated, and the value of M will be constant. The ferromagnetic material could be considered as a permanent magnet. The question is whether there is any interest in using oversaturated ferromagnetic pieces instead of permanent magnets. The response is “yes” if we consider the volume of rare earth, a strategic material necessary to manufacture permanent magnets and the price of which continually increases. We should also consider the process to fix them and their cost in the case of building a large power machine (typically several MW). Compared to classical superconducting machine structures, the cryogenic part of our machine is fixed. The only rotating part will be composed of massive ferromagnetic pieces. In addition, this type of machine is quasi insensitive to the armature reaction, and the recovery of the required magnetization is fast after the disappearance of any default. We also have to take into account that the evolution of new superconducting materials is in “daily” progress, which makes superconducting machines more promising.

However, the main problem is to obtain a source of magnetic field with a high value in a large volume. The solution can be inspired by the expertise found in the domain of static coils used for MRI or for large physics instruments. In any case, it seems to be obvious that superconducting coils constitute the best solution to build the source of magnetic field.

Taking into account all the above considerations, we propose to study the feasibility of an inductor of an oversaturated machine with radial flux density distribution.

3. FROM THE PRINCIPLE TOWARD THE DESIGN

The topology of a radial oversaturated inductor as well as the back iron is schematized in Figure 1. The inductor is composed of regularly distributed massive ferromagnetic pieces magnetized by superconducting coils.

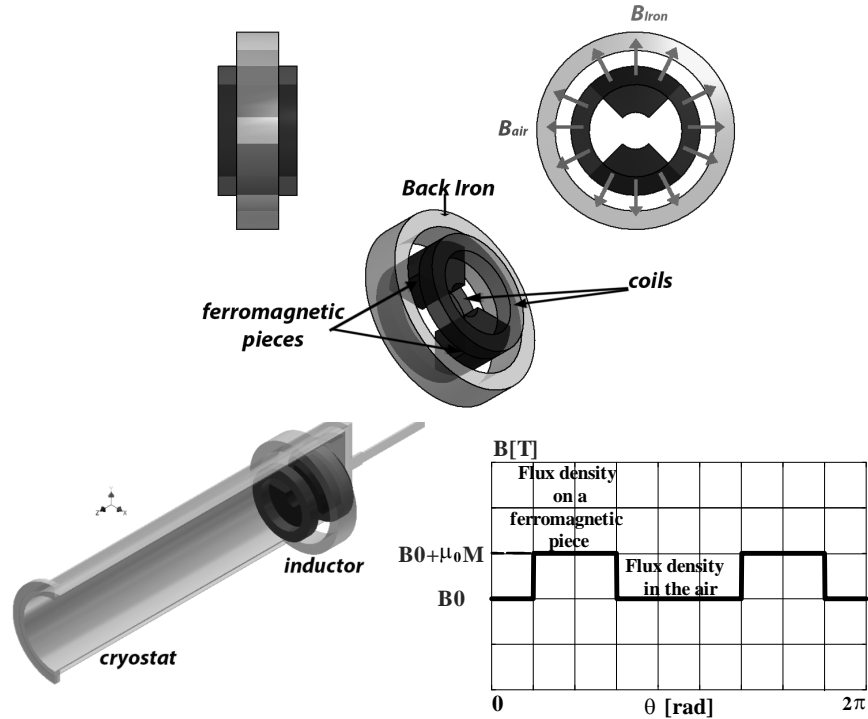


Figure 1. Scheme of the topology of the inductor of the oversaturated superconducting machine.

In this case, we expect to find a square wave flux density distribution around the inductor varying between B_0 and $(B_0 + \mu_0 M)$.

At this point, we would like to draw the attention that in this machine, the torque is not due to the difference between the direct and quadrature inductances, as in a classical reluctance machine. This term, $(L_d - L_q)$, is close to zero when the ferromagnetic pieces are oversaturated. The rotor must be considered as equivalent to a one polarity permanent magnets machine. The calculation of torque or EMF is done in a classical way as for any synchronous machine.

To obtain a sufficiently high value of the flux density, we use two superconducting coils. The armature can be made of copper or superconductors. An environmental confinement of the magnetic field needs a magnetic shield or supplementary coils.

Figure 1 shows that by using two coils, fed by opposite currents, we obtain a magnetic field with a radial component in the volume confined between them. It is important to note that a final design consists of superconducting coils with their individual cryostat and an armature composed of copper or superconductor winding with its own cryostat. The only rotating part is the one composed of magnetically oversaturated ferromagnetic pieces.

To conclude, one can highlight the potential advantages of the proposed axial and radial structures: the coils are static and consequently need a very simple cryogenic system compared to those used to cool down a rotating part, which is the case for many superconducting machines. The armature winding is also static and can be composed of copper or superconductors. Consequently, the only rotating part is the one composed of ferromagnetic pieces which is very robust as demonstrated with an axial structure studied and tested [7, 8].

The study of the inductor, composed of superconducting coils and oversaturated ferromagnetic pieces, is presented in this paper. The magnetic field distribution, firstly determined in a theoretical study, will need experimental validation.

4. DESIGN OF AN INDUCTOR

4.1. Assumptions

The first problem to consider in this topology is to generate a high magnetic field in a relatively large volume to oversaturate ferromagnetic pieces. This can be assured using superconducting coils. Operating below their critical temperature, such coils can transport current densities high enough to generate the needed magnetic field. Such advantages are accompanied with cooling problems, but several solutions can be considered (liquid helium or nitrogen, cryo-cooler). Considering the prices of superconducting wires, NbTi superconductor is chosen and will be cooled by liquid helium.

To make the cryogenic process easy to implement, all the parts of the apparatus are static and will be put in an existing cryostat, thus its internal diameter constitutes a limit for the dimensions of the superconducting coils and the inductor.

The total length of the inductor is limited so that it has enough volume of liquid helium to cool down the system

4.2. Description of the Inductor

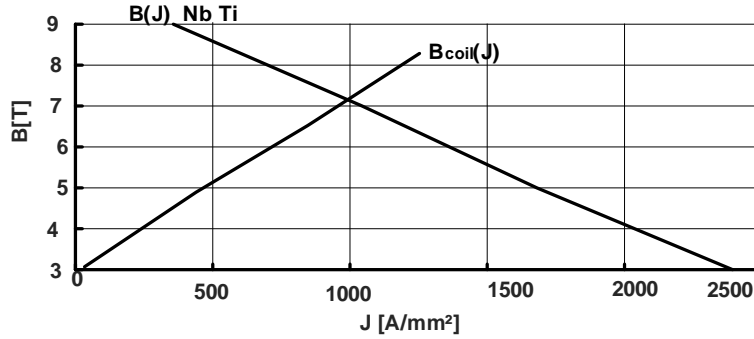
The system of coils and ferromagnetic pieces, arranged according to Figure 1, creates, at the level of the armature winding, an angular variation of the magnetic flux density. The oversaturation prevents, in addition, the demagnetization caused by the armature winding reaction.

The design of the experimental bench consists of calculating the superconducting coils and the size of the ferromagnetic pieces. We also add the external back iron because it is an important part for the design of the inductor. All the parts for this probative apparatus are static.

The coils are made of a low temperature superconducting wire (NbTi). The design of the coil must take into account the $B(J)$ law of the superconducting wire at an operating temperature. For an air core coil system, the operating current density represents the point of intersection between the load line of the coils and the characteristics of the superconducting wire (see Figure 2). The load line $B_{coil}(J)$ is the maximum of the flux density inside the coils as a function of the current density. We should notice that adding ferromagnetic pieces changes the magnetic flux distribution inside the coils. As these ferromagnetic pieces are oversaturated, their behavior is linear, but the behavior of the back iron is not

Table 1. NbTi wire characteristics.

| | |
|-------------------------|---------------------|
| supplier | SUPERCON INC |
| Reference | 56S53Multi filament |
| Number of filaments | 56 |
| Filament diameter | 48 μm |
| Bare wire diameter | 0.50 mm |
| Insolated wire diameter | 0.54 mm |
| Cu/Su ratio | 0.9 : 1 |

**Figure 2.** NbTi $B(J)$ Law.

linear. This point constitutes a difficult problem to solve in the design. The characteristics of the used superconducting wire are mentioned in Table 1 and Figure 2.

In the upcoming sections, we present a first topology that represents the oversaturated superconducting radial machine inductor designed for the chosen cryostat. This topology, at those conditions, show a low flux density variation at the armature windings. A second topology is then presented after a coils shape analysis. It consists of a new shape of coils and ferromagnetic pieces inside and outside the cryostat to increase the flux density variation at the armature winding.

4.3. First Topology

Taking into account the constraints cited above. The dimensions, in reference to Figure 3, are mentioned in Table 2. The value of the used current density is chosen so that we reach, for the operating temperature, a maximum value using $B(J)$ law of our superconducting wire.

The distance between the coils represents the active length of the armature winding. This distance should be a result of a compromise between the volume of the energy conversion medium, which must remain sufficient, and the value of the radial flux density, which must maintain the orientation of the magnetic moments. The dimensions must reflect the compromises and choices to maximize the $\Delta B \times L$ product at the armature winding while taking into account the geometric constrains of this experimental bench (see Figure 4). Increasing the product $\Delta B \times L$ increases the torque of the machine.

Considering the nonlinearities of the problem and taking into account the assumptions presented in the previous section, the dimensions of this first topology are the results of a non-exhaustive parametric study on the coils and ferromagnetic pieces (see Table 2).

The computations are performed by using finite element software [9], with a nonlinear $B(H)$ curve for all ferromagnetic pieces. It leads to the results presented in Figure 4. In this case, the computed current density is 500 A/mm².

In order to verify the oversaturation criterion, we visualize the magnetic flux inside the ferromagnetic piece along the r -axis, as illustrated in Figure 3. Figure 4(a) represents the variation of the flux density on radial line passing through the ferromagnetic piece at $z = L/2$. The two vertical

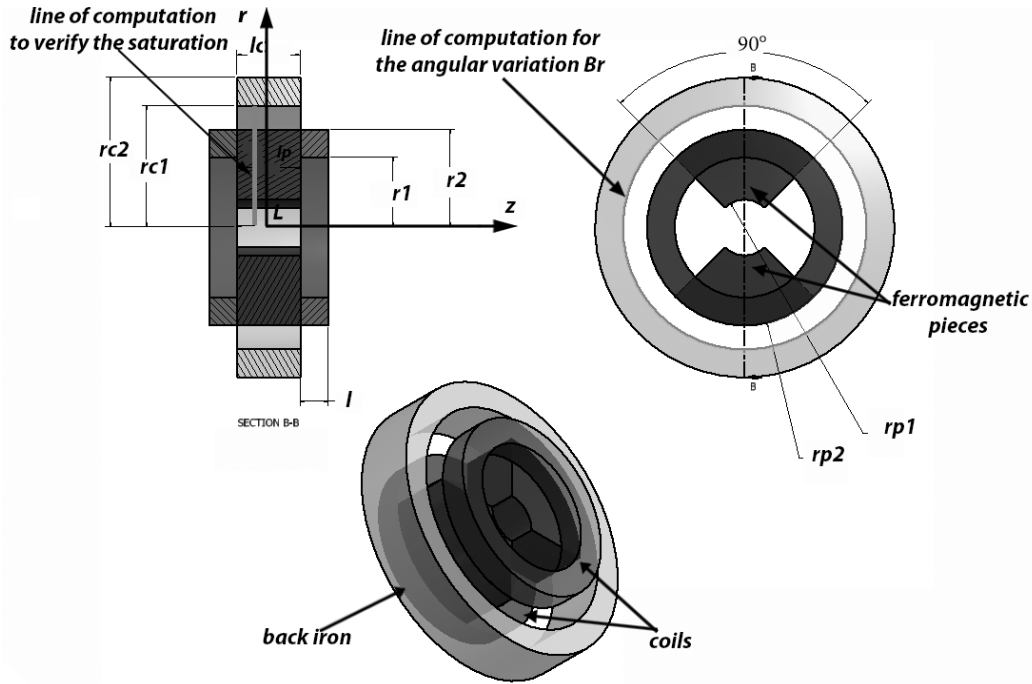


Figure 3. Scheme of the first topology.

Table 2. Dimensions (Figures 2–3).

| | |
|---------------|------------|
| $r1$ mm | 53 |
| $r2$ mm | 72 |
| l mm | 45 |
| L mm | 70 |
| $rp1$ mm | 20 |
| $rp2$ mm | 72 |
| θ_{fe} | 90° |
| lc mm | 70 |
| $rc1$ mm | 89 |
| $rc2$ mm | 129 |

lines delimit the space occupied by the ferromagnetic piece. The latter is clearly oversaturated because the value of the magnetic flux inside it largely exceeds 2 T.

Now that the criterion of saturation is verified, we can see in Figure 4(b) the variation of the angular radial magnetic flux density at the surface of the inductor, $r = rp2$. This variation is about $\Delta B(rp2) = 1$ T. These results validate the principle of the oversaturated machine.

The variation of Br , at $r = rc1$, 17 mm far away from the inductor, where the future armature windings will be located, is about $\Delta B(rc1) = 0.7$ T. We note that the variation diminishes. This is due to the large air gap imposed by the cryostat of this probative bench. One can note that this problem is avoided in a complete machine, with a classical room temperature armature, because the air gap can be shortened to a few millimeters as in a classical machine. However, due to the large air gap the amplitude of the space harmonics decreases drastically, and this is an undeniable advantage. If the project deals with a machine with a superconducting armature, the large air gap is inevitable, and improvements must be brought to the design.

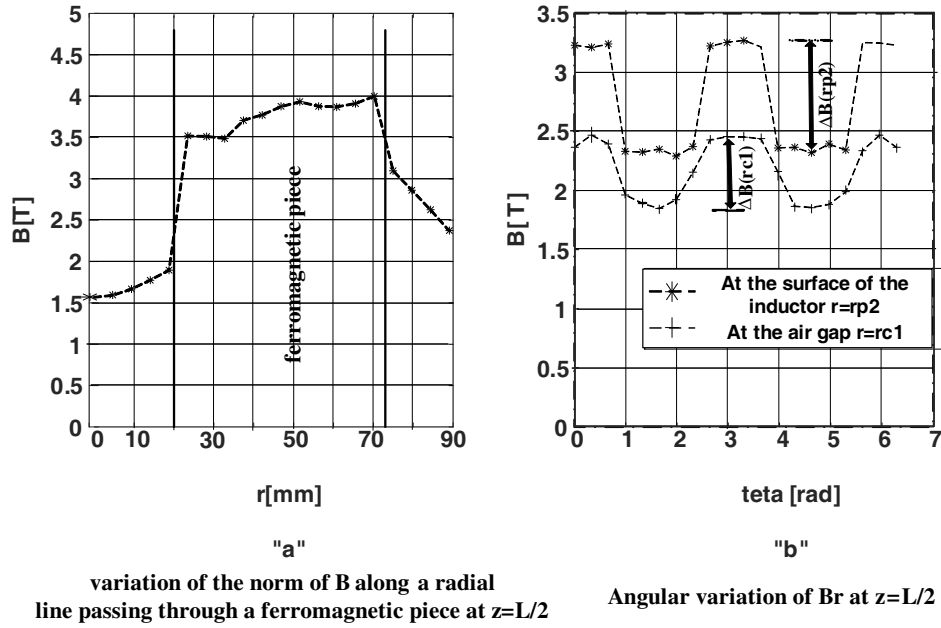


Figure 4. Results of computations on the first topology.

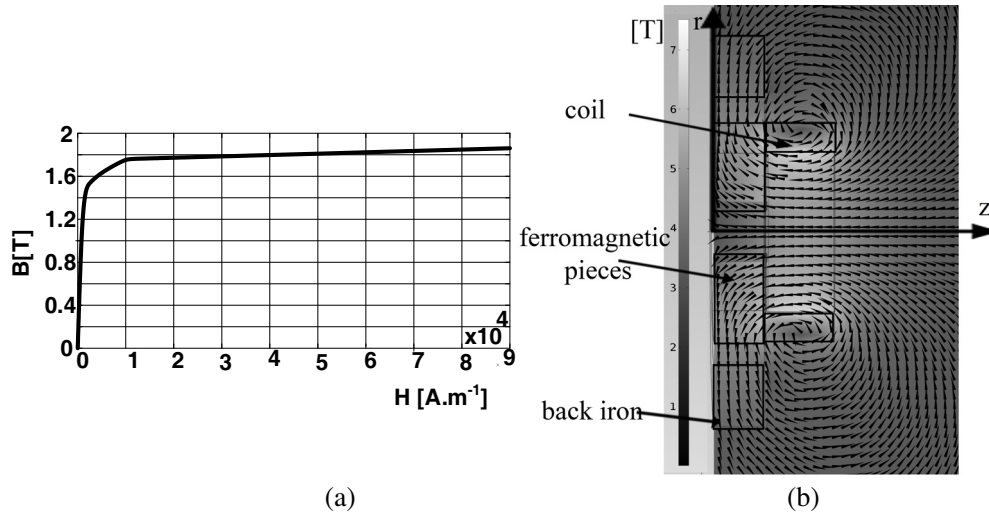


Figure 5. Flux lines and $B(H)$ curve of the used ferromagnetic material.

Considering the $B(H)$ curve of the used ferromagnetic material (see Figure 5(a)), we expect to have an angular variation of $Br(\theta)$, at the surface of the ferromagnetic pieces $r = rp2$, of around 1.8 T. Unfortunately, as shown in Figure 4(b), we only obtain a Br variation of 1 T. The difference is explained by the fact that the superconducting coils generate a magnetizing field oriented in the (r, z) plan as shown in Figure 5(b). To increase the ratio Br/Bz , we perform a coil shape analysis. This analysis is specifically made for this experimental bench with its geometric constraints. A shape analysis for a large machine will have the same purpose, but the approach will be adapted for other types of constraints.

4.4. Coils Shape Analysis

Taking into account the large air gap, we present the analysis that leads to finding an excitation system able to obtain a flux density with a value as high as possible at the armature. To overcome the

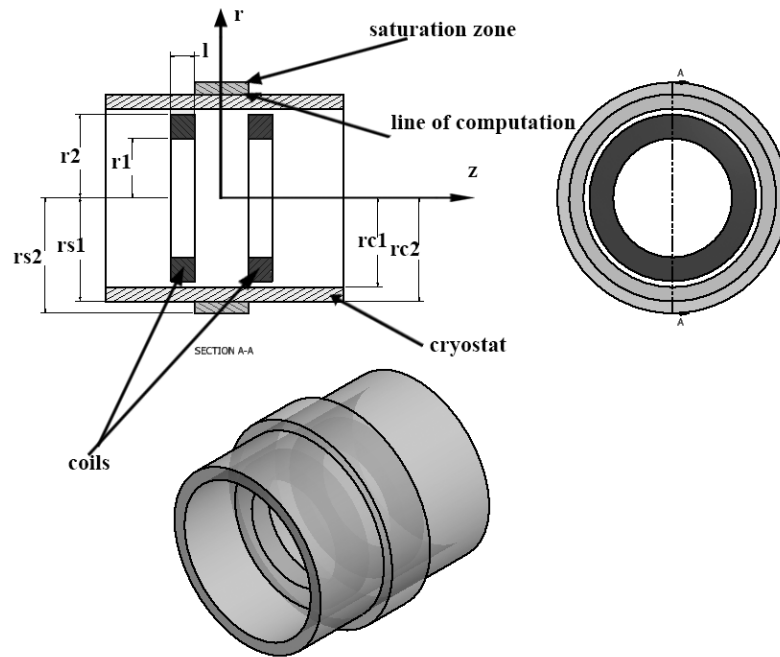


Figure 6. Scheme showing the saturation zone.

problem caused by the large air gap, we can oversaturate the ferromagnetic pieces outside the cryostat. To remedy to the problem caused by the orientation of the magnetizing field, we perform a coil shape analysis to create a radial saturating magnetic field outside the cryostat, in the region where the external ferromagnetic pieces will be placed. We call this region the saturation zone (see Figure 6). We mention that there exist in the literature some studies on superconducting coils shapes in which criteria are mainly to increase the current density [10].

Till now, the excitation system is formed by superconducting coils of a rectangular cross sectional area. The maximum current density that can be carried by the coils is limited by the $B(J)$ curve of the superconductor. For an operating temperature, the current density depends on the shape and position of each magnetic component (coils, ferromagnetic pieces and back iron).

Our goal is to generate the largest radial component of the magnetic field outside the cryostat in a region that happens to be situated away from the external radius of the coils.

The main idea is to play on the shape of the cross sectional area of the superconducting coil, knowing that any modification on the shape results in a change of the current density allowed in the superconductor as well as the orientation of the flux lines.

Figure 7 shows the basic cross sections we chosen for the study (shape “a”, “b” and “c”). For each cross section shape, we compute the maximum current density allowed by such geometries and use it to compute the magnetic field along the external vessel of the cryostat, at $r = rs1$ (see Figure 6).

Our investigations to enhance the radial flux density component along the computation line in Figure 6 lead us to studying shapes that are combinations of the basic ones, “b” and “c”.

The external radius of each shape is fixed by the cryostat radius $r2$. The distance between the two coils is the same for all configurations and is 70 mm.

The shapes are presented in Figure 7. Table 3 mentions the variable parameters of shapes “a”, “b” and “c”.

For each configuration presented in Figure 7, we compute the maximum current density allowed by the superconducting coil. Afterwards, we use the latter to compute the radial magnetic flux density and the orientation of \mathbf{B} relatively to the radial axis at the line of computation in Figure 6.

Considering the symmetry of the structure, we perform the computations only on half of the machine, between 0 and $-L/2$ along the z axis. The results of computations are presented in Figure 8.

Shape “a” is a squared cross sectional area, and we notice that its current density is about

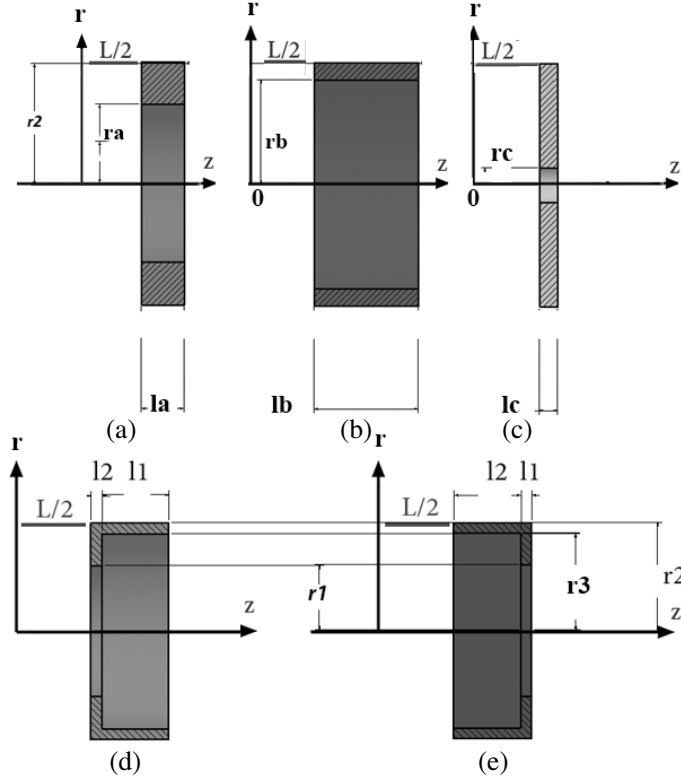


Figure 7. Shapes of the superconducting coils for a new topology.

Table 3. Dimensions of shapes “a”, “b” and “c”.

| Basic shapes | ra [mm] | la [mm] | rb [mm] | lb [mm] | rc [mm] | lc [mm] |
|-------------------------------|-----------|-----------|-----------|-----------|-----------|-----------|
| | | 47.5 | 24.5 | 62 | 60 | 12 |
| Dimensions for shapes “d” “e” | | $r1$ [mm] | $r2$ [mm] | $r3$ [mm] | $l1$ [mm] | $l2$ [mm] |
| “e” | | 12 | 72 | 62 | 10 | 60 |
| “d” | | 12 | 72 | 62 | 60 | 10 |

$Ja = 234 \text{ A/mm}^2$. The radial component is around 0.6 T along the z axis and is far from reaching an over saturating value. The orientation of \mathbf{B} can reach more than 20° at $z = -20 \text{ mm}$.

Shapes “b” and “c” have the same surface as that of shape “a”. We obtain them by changing the ratio between the length and width of shape “a”.

Shape “c” is large along the radial direction, and we notice that its maximum current density is about $Jc = 433 \text{ A/mm}^2$ and is higher than that of shape “a”; however, the amplitude of the radial component and the angle between the flux density vector \mathbf{B} and the radial axis indicate that the flux lines created by the latter, in the region of magnetization, are mainly oriented along the z axis.

Shape “b” is large along the z -direction; we notice that its maximum current density is lower than that of shapes “a” and “c”; however, its radial component is the highest. This is explained by the fact that its deviation from the radial direction is the lowest.

So far, shape “b” is the best candidate to meet our considerations; unfortunately, the amplitude of the radial component is too low to oversaturate a ferromagnetic material.

Although the coils have the same distance between them and the same cross sectional area surface, a change in the ratio between the length and width of the surface changes the maximum current density allowed in the coil. This is because the changes in shape change the distribution of the flux lines, so the maximum of B inside the coil can be lowered or increased.

After this brief analysis, we want to get the advantages of both shapes “b” and “c”. The idea is to combine the two shapes to get a more radial flux density by superposing both of their flux lines. The two simple possible configurations are presented as shapes “d” and “e”.

We notice that shape “d” has a higher current density and higher amplitude of the radial component than shape “e”; however, shape “e” has a more radial orientation (see Figure 8).

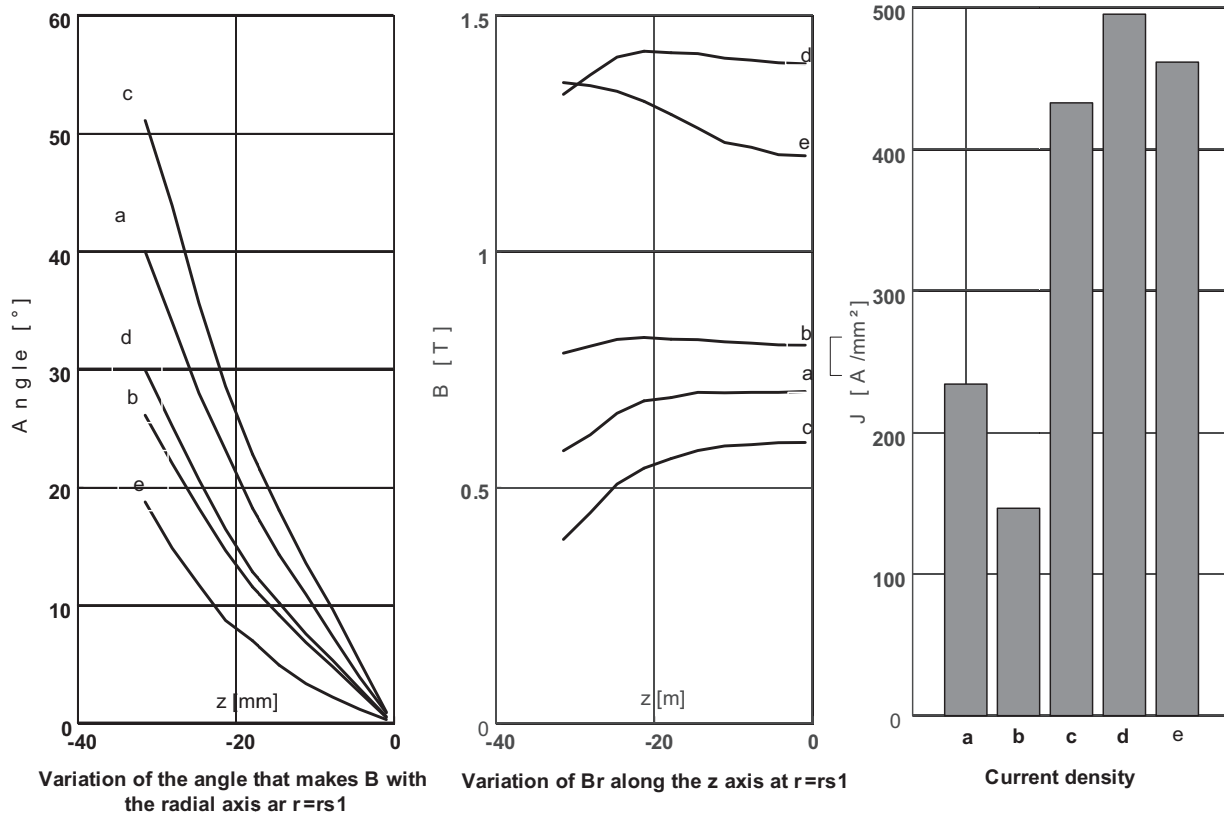


Figure 8. Results of computations for different coil shapes.

Choosing shape “e”, we notice that the amplitude of the radial flux density is ranging between 1.2 and 1.4 T. This is the limitations of this configuration with the geometric sizing constraints.

4.5. Second Topology

In the previous part, we have considered the coils alone in the space. A structure of an inductor is more complicated, and its final design becomes difficult.

To reach an over saturating value outside, in the region of magnetization, we can use ferromagnetic pieces between the coils inside the cryostat. Their role is to increase the amplitude of the radial component of configuration “e” to permit an oversaturating value in the predefined region of magnetization.

At this point, the topology is well defined: two superconducting coils with the shape of configuration “e”. Between those coils we place ferromagnetic pieces. Outside the cryostat we place another set of ferromagnetic pieces. The latter have to be oversaturated with the magnetic field created by the coils and inner pieces (see Figure 9).

4.6. Parametric Study

To generate a saturating magnetic field for the ferromagnetic pieces while increasing the product $\Delta B \times L$ at the level of the armature, we perform a parametric study on the parameters of the machine (see

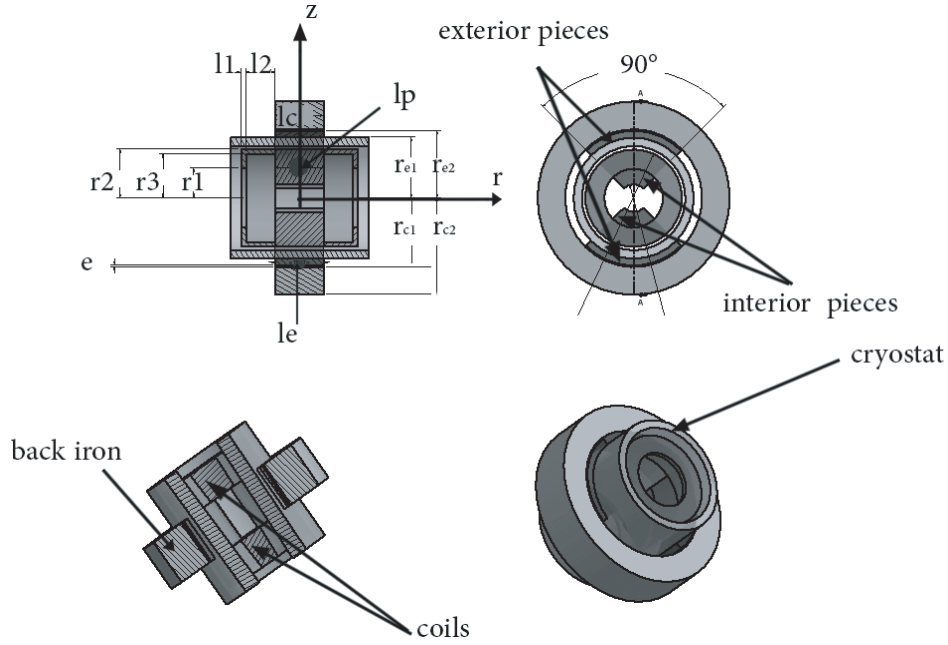


Figure 9. Second topology scheme.

Figure 9). The only fixed parameters are the outer radius of the inductor limited by the cryostat and the distance L between the superconducting coils. Table 4 mentions the parameters and precisely the ones that were varied and the ones that were fixed. Not forgetting that for each set of parameters we find a new maximum value of current density.

The parametric study yields a huge number of results that need analysis and treatment to get the desired results. The fruit of such a study is presented in Table 4 in reference to Figure 9.

Table 4. Dimensions of the second topology.

| | Model's parameters | |
|------------------------------------|--------------------|-----|
| Varied during the parametric study | $r1$ [mm] | 55 |
| | $r3$ [mm] | 63 |
| | $l1$ [mm] | 27 |
| | $l2$ [mm] | 63 |
| | J [A/mm^2] | 660 |
| | $rp1$ [mm] | 20 |
| | $rp2$ [mm] | 72 |
| | lp [mm] | 70 |
| | $re1$ [mm] | 87 |
| | $re2$ [mm] | 97 |
| | le [mm] | 118 |
| | $rc1$ [mm] | 99 |
| | $rc2$ [mm] | 139 |
| | lc [mm] | 70 |
| Fixed during the parametric study | $r2$ [mm] | 72 |
| | L [mm] | 70 |
| | e [mm] | 2 |

The results of computations are the subject of Figure 10. The obtained current density is 660 A/mm^2 .

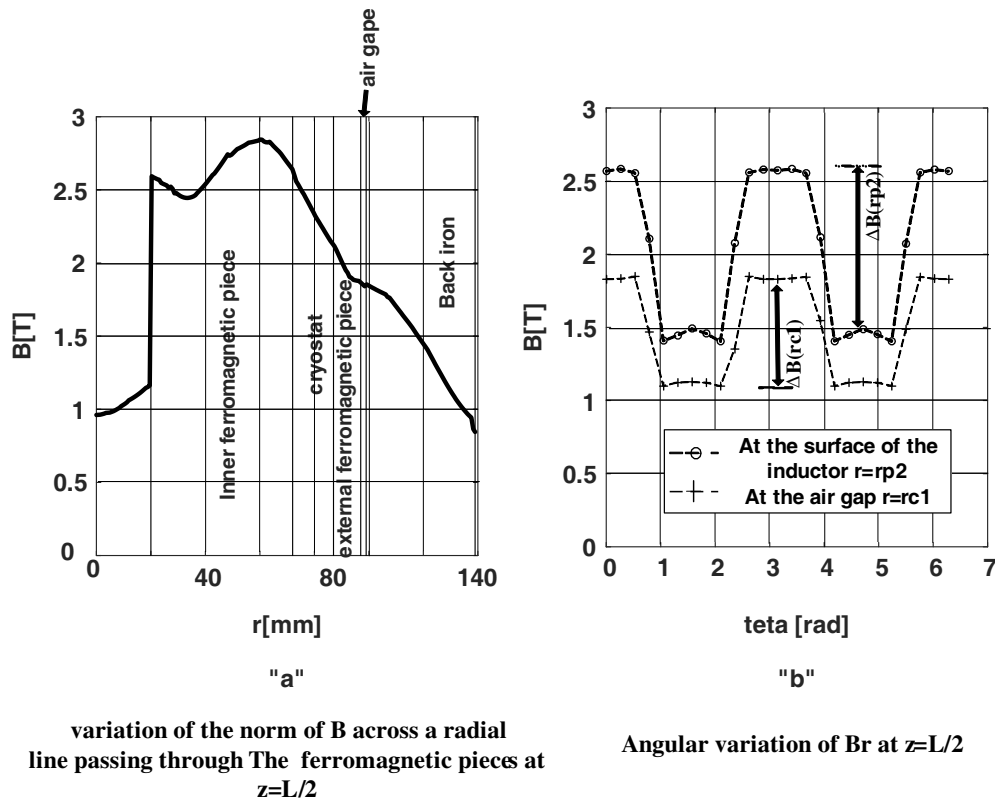


Figure 10. Results of computations on the second topology.

Figure 10(a) shows the results of computations performed on a radial line passing through the middle of the ferromagnetic piece at $z = L/2$; we notice that the inner pieces are oversaturated. The outer pieces are sufficiently magnetized.

Figure 10(b) represents the variation of the radial flux density at the surface of the inductor, $r = rp2$, and at the inner surface of the back iron, $r = rc1$, at ($z = L/2$).

We note that the variation of the flux density at the surface of the inductor, $r = rp2$, is higher than that obtained in the first topology and is about $\Delta B(rp2) = 1.3 \text{ T}$. This is due to the new shape of superconducting coils as well as the contribution of the outer ferromagnetic piece. We also notice that the variation of the angular flux density at the armature winding, $r = rc1$, has also increased and is about $\Delta B(rc1) = 1 \text{ T}$ for the fundamental. This shows the benefits of using two sets of ferromagnetic pieces.

5. INDUCTOR MANUFACTURE

Thanks to the obtained results, an experimental part is now under development as shown in Figure 11. To achieve that, additional constraints must be taken into account. First of them deals with the acting magnetic forces between the components of the inductor, and the others concern the thermal losses due to Joule effect in the electric connection cables of the superconducting coils. High temperature superconducting current leads are planned to be used to reduce the above mentioned losses and consequently the liquid helium consumption.

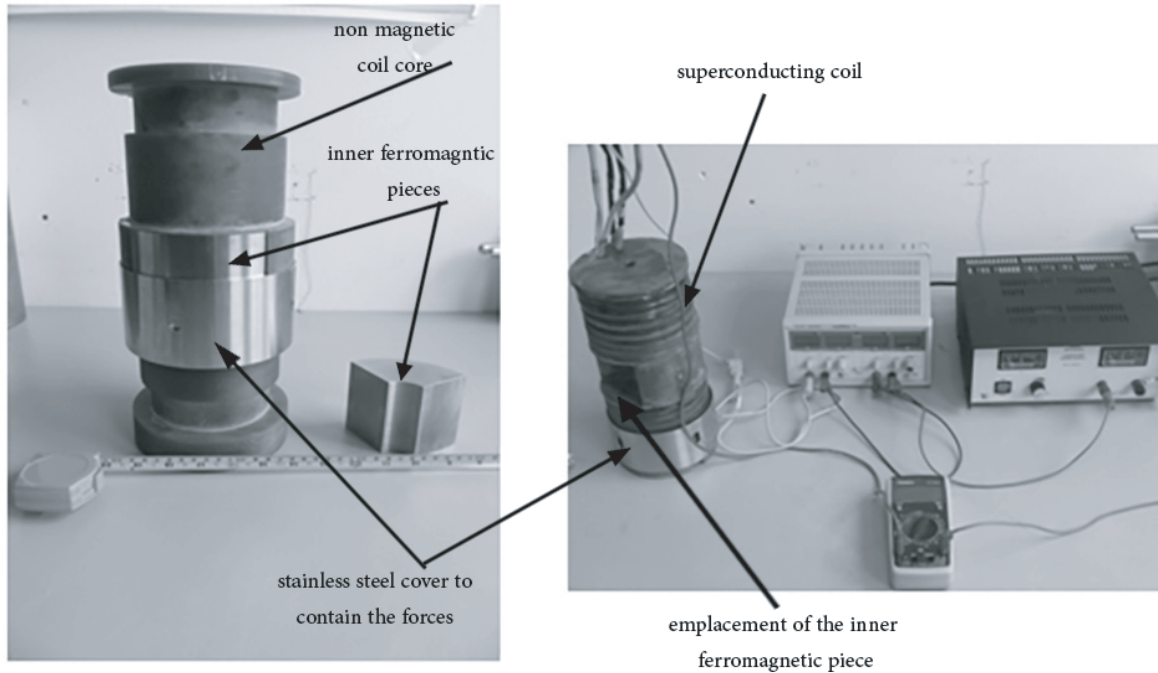


Figure 11. Pictures of the inductor under construction.

6. CONCLUSION

This paper contributes to the design of a new topology of electrical superconducting machine of a radial flux density using oversaturated ferromagnetic pieces. This work presents the study of an inductor for an experimental bench. The aim of the work is to verify and illustrate the principle and compute the inductor air gap flux density.

The design of the experimental bench highlights the problems encountered to build such a machine and lays out the tools that can help to study the design of large power superconducting oversaturated radial machine.

Considering the constraints on the dimensions, such as the large air gap caused by the cryostat, variation of the angular magnetic flux density of the first topology is relatively small and is about 0.75 T.

To increase the inductor air gap flux density, a coils shape analysis is performed and allowed to conclude that the “L” shape constitutes a suitable solution, for this range of parameters, and enhances the radial component of the magnetic field, even away from the external radius of the coils themselves.

Ferromagnetic pieces are placed inside and outside the cryostat. This configuration allows us to place an armature winding with an air gap as small as the one of conventional machines, 2 mm in our case.

The parametric study allows us to find the dimensions that result in a mainly radial magnetic flux density in the region of magnetization.

REFERENCES

1. Ailam, E. H., D. Netter, J. Leveque, B. Douine, P. J. Masson, and A. Rezzoug, “Design and testing of a superconducting rotating machine,” *IEEE Transactions on Applied Superconductivity*, Vol. 17, No. 1, 27–33, March 2007.
2. Lin, F., R. Qu, and D. Li, “A novel fully superconducting geared machine,” *IEEE Transactions on Applied Superconductivity*, Vol. 26, No. 7, 1–5, October 2016.

3. Lin, F., R. H. Qu, and D. W. Li, "Topologies for fully superconducting machines," *2015 IEEE International Conference on Applied Superconductivity and Electromagnetic Devices (ASEMD)*, 496–497, Shanghai, 2015.
4. Jeong, J. S., D. k. An, J. P. Hong, H. J. Kim, and Y. S. Jo, "Design of a 10-mw-class HTS homopolar generator for wind turbines," *IEEE Transactions on Applied Superconductivity*, Vol. 27, No. 4, 1–4, June 2017.
5. Kawamura, M. and J. A. Jones, "Superconducting super motor and generator," *IEEE Transactions on Applied Superconductivity*, Vol. 27, No. 4, 1–5, June 2017.
6. Rezzoug, A. and M. El-Hadi Zaïm, *Non-conventional Electrical Machine*, 191–255, ISTE Ltd and John Wiley & Sons, Inc, Great Britain-United States, 2012.
7. Rezzoug, A., A. Mailfert, and P. Manfe, "Cryogenic supersaturated synchronous machine optimization and first experiment results," *IEEE Transactions on Magnetics*, Vol. 20, No. 5, 1795–1797, September 1984.
8. Manfe, P., A. Rezzoug, A. Mailfert, H. Desportes, J. Lottin, and C. Leschevin, "Prototype 'Supersat 001 — Probative results'," *IEEE Transactions on Magnetics*, Vol. 23, No. 6, 3903–3907, November 1987.
9. www.comsol.com.
10. Jiang, Z. Q. and J. X. Jin, "Investigation of step-shaped field coil for large capacity superconducting motors," *IEEE International Conference on Applied Superconductivity and Electromagnetic Devices (ASEMD)*, 11–12, Shanghai, 2015.